
E-MCTS: Deep Exploration in Model-Based Reinforcement Learning by Planning with Epistemic Uncertainty

Yaniv Oren, Matthijs T. J. Spaan & Wendelin Böhmer

Delft University of Technology

2628 CD Delft, the Netherlands

{y.oren, m.t.j.spaan, j.w.bohmer}@tudelft.nl

Abstract

One of the most well-studied and highly performing planning approaches used in Model-Based Reinforcement Learning (MBRL) is Monte-Carlo Tree Search (MCTS). Key challenges of MCTS-based MBRL methods remain dedicated deep exploration and reliability in the face of the unknown, and both challenges can be alleviated through principled epistemic uncertainty estimation in the predictions of MCTS. We present two main contributions: First, we develop methodology to propagate epistemic uncertainty in MCTS, enabling agents to estimate the epistemic uncertainty in their predictions. Second, we utilize the propagated uncertainty for a novel deep exploration algorithm by explicitly planning to explore. We incorporate our approach into variations of MCTS-based MBRL approaches with learned and provided models, and empirically show deep exploration through successful epistemic uncertainty estimation achieved by our approach. We compare to a non-planning-based deep-exploration baseline, and demonstrate that planning with epistemic MCTS significantly outperforms non-planning based exploration in the investigated setting.

1 Introduction

Model-based reinforcement learning (MBRL) has shown tremendous achievements in recent years, from super-human performance in games [Schrittwieser et al., 2020, Silver et al., 2018], to outperforming human designers in tasks that previously relied on intricate human engineering [Mandhane et al., 2022]. MBRL algorithms most commonly leverage their model (whether it is dynamically learned as part of the RL task, or pre-specified to the agent) for planning [Moerland et al., 2023]. Some of the best performing planning-based MBRL approaches, Mu/AlphaZero [Schrittwieser et al., 2020, Silver et al., 2018] rely on Monte-Carlo Tree Search (MCTS), a structured, extensively researched and commonly used planning approach. While the final performance that has been demonstrated with these algorithms is record-breaking, they are notoriously expensive to train, in compute as well as in samples. They are also unable to estimate the epistemic uncertainty in their predictions, preventing them from being reliable in the face of the unknown. A common approach for improving sample efficiency is through improved exploration. Exploration approaches range from uninformed random-action-selection based (such as employed by Alpha/MuZero) to more advanced approaches, such as exploration bonuses based on epistemic uncertainty, which incentivize future visitations to states and actions that are expected to result in new knowledge.

Effective epistemic uncertainty estimation in the predictions of the agent can be used to improve in both areas of challenge: reliability in the face of the unknown and advanced exploration. Further, planning for exploration promises to harness the benefits of planning (such as improved value

estimation and better action selection) explicitly for exploration, an idea which was previously explored by Sekar et al. [2020] with promising results.

In this work, we develop methodology to 1) incorporate epistemic uncertainty into MCTS, enabling agents to estimate the epistemic uncertainty associated with predictions at the root of the MCTS planning tree (**Epistemic-MCTS**) and 2) leverage the uncertainty for deep exploration that capitalizes on the strengths of planning, by modifying the MCTS objective to an exploratory objective. We evaluate our agent on the benchmark hard-exploration task of Deep Sea [Osband et al., 2020] against exploration baselines that do not leverage planning. In our experiments, our agent demonstrates deep exploration and significantly outperforms both naive and sophisticated exploration baselines.

The remainder of this paper is organized as follows: Section 2 provides relevant background for MBRL, MCTS and epistemic uncertainty estimation in deep RL. Section 3 describes our contributions, starting with the framework for uncertainty propagation in MCTS (E-MCTS), followed by our approach for harnessing E-MCTS to achieve deep exploration and a discussion regarding the challenges of estimating epistemic uncertainty in planning with an abstracted, learned model of the environment. Section 4 discusses related work. Section 5 evaluates our method with different dynamics models against a hard-exploration benchmark and compares to standard exploration baselines. Finally, Section 6 concludes the paper and discusses future work.

2 Background

2.1 Model-Based Reinforcement Learning

In RL, an agent learns a behavior policy $\pi(a|s)$ through interactions with an environment, by observing states (or observations), executing actions and receiving rewards. The environment is represented with a Markov Decision Process [MDP, Bellman, 1957], or a partially-observable MDP [POMDP, Åström, 1965]. An MDP \mathcal{M} is a tuple: $\mathcal{M} = \langle \mathcal{S}, \mathcal{A}, \rho, P, R \rangle$, where \mathcal{S} is a set of states, \mathcal{A} a set of actions, ρ the initial state distribution,

$R : \mathcal{S} \times \mathcal{A} \times \mathcal{S} \rightarrow \mathbb{R}$ a bounded reward function, and $P : \mathcal{S} \times \mathcal{A} \times \mathcal{S} \rightarrow [0, 1]$ is a transition function, where $P(s_{t+1}|s_t, a_t)$ specifies the probability of transitioning from state s_t to state s_{t+1} after executing action a_t at time t . In a POMDP $\mathcal{M}' = \langle \mathcal{S}, \mathcal{A}, \rho, P, R, \Omega, O \rangle$, the agent observes observations $o_t \in \Omega$. $O : \mathcal{S} \times \mathcal{A} \times \Omega \rightarrow [0, 1]$ specifies the probability $O(o|s_t, a_t)$ of observing o . In MBRL the agent uses a model of the environment to optimize its policy, often through planning. The model is either learned from interactions, or provided. In Deep MBRL (DMBRL) the agent utilizes deep neural networks as function approximators. Many RL approaches rely on learning a state-action *Q-value function* $Q^\pi(s, a) = \mathbb{E}[R(s, a, s') + \gamma V^\pi(s') | s' \sim P(\cdot|s, a)]$ or the corresponding state *value function* $V^\pi(s) = \mathbb{E}[Q^\pi(s, a) | a \sim \pi(\cdot|s)]$, which represents the expected return from starting in state s (and possibly action a) and then following a policy $\pi(a_t|s_t)$ which specifies the probability of selecting the action a_t in state s_t . The discount factor $0 < \gamma < 1$ is used in infinite-horizon (PO)MDPs to guarantee that the values remain bounded, and is commonly used in RL for learning stability.

2.2 Monte Carlo Tree Search

MCTS is a planning algorithm that constructs a planning tree with the current state s_t at its root to estimate the objective: $\arg \max_a \max_\pi Q^\pi(s_t, a)$. The algorithm iteratively performs *trajectory selection, expansion, simulation and backup* to arrive at better estimates at the root of the tree. At each planning step i , starting from the root node $s_{t,0}^i \equiv \hat{s}_0$, the algorithm selects a trajectory in the existing tree based on the averaged returns $q(\hat{s}_k, a)$ experienced in past trajectories selecting the action a in the same node \hat{s}_k , and a search heuristic, such as an Upper Confidence Bound for Trees [UCT, Kocsis and Szepesvári, 2006]:

$$a_k = \arg \max_{a \in A} q(\hat{s}_k, a) + 2C_p \sqrt{\frac{2 \log(\sum_{a'} N(\hat{s}_k, a'))}{N(\hat{s}_k, a)}}, \quad (1)$$

where $N(\hat{s}_k, a)$ denotes the number of times action a has been executed in node \hat{s}_k , and $C_p > 0$ trades off exploration of new nodes with maximizing observed return. When the the trajectory selection arrives at a leaf node \hat{s}_T MCTS expands the node and estimates its initial value as the average of Monte-Carlo rollouts using a random policy. Recent DMBRL algorithms that use MCTS

such as Alpha/MuZero [Silver et al., 2017] replace the rollouts with a value function $v(\hat{s}_T)$ that is approximated by a neural network and use the PUCT [Rosin, 2011] search heuristic instead of UCT:

$$a_k = \arg \max_{a \in A} q(\hat{s}_k, a) + \pi(a|\hat{s}_k) C_p \frac{\sqrt{\sum_{a'} N(\hat{s}_k, a')}}{1 + N(\hat{s}_k, a)}. \quad (2)$$

Where $\pi(a|\hat{s}_k)$ is either given, or learned by imitating the MCTS policy π^{MCTS} , to incorporate prior knowledge into the search. MCTS propagates the return (discounted reward for visited nodes plus leaf's value) back along the planning trajectory. At the root of the tree, the optimal value $\max_{\pi} V^{\pi}(s_t)$ of current state s_t is estimated based on the averaged returns experienced through every action a , and averaged over the actions:

$$\max_{\pi} V^{\pi}(s_t) \approx \sum_{a \in \mathcal{A}} \frac{N(\hat{s}_0, a)}{\sum_{a' \in \mathcal{A}} N(\hat{s}_0, a')} q(\hat{s}_0, a) =: \sum_{a \in \mathcal{A}} \pi^{\text{MCTS}}(a|s_t) q(\hat{s}_0, a) =: v_t^{\text{MCTS}}. \quad (3)$$

2.3 MCTS-Based MBRL

MCTS requires access to three core functions. Those are: (i) a representation function $g(s_t) = \hat{s}_0 \in \hat{\mathcal{S}}$ that encodes the current state at the root of the tree into a latent space, in which (ii) a transition function $f(\hat{s}_k, a_k) = \hat{s}_{k+1}$ predicts the next latent state and (iii) a function $r(\hat{s}_k, a_k) = \mathbb{E}[r_k|\hat{s}_k, a_k]$ that predicts the corresponding average reward. Note that for an identity function $g(s_t) = s_t$ all models, functions and policies would be defined in the true state space \mathcal{S} , and that in a POMDP g can encode the current observation o_t or the entire action-observation history $\langle o_0, a_0, o_1, a_1, \dots, o_t \rangle$. As in Mu/AlphaZero [Schrittwieser et al., 2020, Silver et al., 2018], a value function $v(\hat{s}_T)$ can be learned for replacing rollouts, and a policy function $\pi(a|\hat{s}_k)$ imitates the MCTS policy to bias planning towards promising actions based on prior knowledge. In deep MBRL (DMBRL) these functions are learned with deep neural networks.

Five common learning signals are used to train the transition model f with varying horizons k :

- 1) A reconstruction loss $L_{re}^k(h(\hat{s}_k), s_{t+k})$, training a decoder h to reconstruct true states s_{t+k} from latent representations \hat{s}_k that have been predicted from $\hat{s}_0 = g(s_t)$, shaping both g and f .
- 2) A consistency loss $L_{co}^k(\hat{s}_k, g(s_{t+k}))$, training the model that predicted states should align with latent representation of states s_t (or observations/histories in POMDP). Critically, L_{co}^k is not used to train g , only f . When the representation function g is an identity, L_{re}^k and L_{co}^k can be thought of as providing the same learning signal. Otherwise, they can be used independently or in combination.
- 3) A reward loss $L_r^k(r(\hat{s}_k, a_k), r_{t+k})$, where the model is trained to predict representations that enable predictions of, and are aligned with, the true rewards observed in the environment r_t .
- 4) A value loss $L_v^k(v(\hat{s}_k), v_{t+k}^{\text{MCTS}})$ that similarly trains the model to predict states that enable value learning.
- 5) A policy loss $L_{\pi}^k(\pi(\cdot|\hat{s}_k), \pi^{\text{MCTS}}(\cdot|s_{t+k}))$ that trains prior policy π to predict the MCTS policy.

These losses are described in more detail in Appendix B.2.

2.4 Estimating Epistemic Uncertainty in Deep Reinforcement Learning

Predictive epistemic uncertainty refers to any uncertainty that is associated with a prediction and is sourced in lack-of-information. For example, prior to repeated tosses of a coin, there can be high uncertainty whether the coin is fair or not. The more the coin has been tossed, the more certain we can be about the coin's fairness, even if we will always retain uncertainty in the exact prediction of heads or tails, without access to a precise simulation of the physics of the coin toss (referred to as *aleatoric* uncertainty, or the inherent stochasticity of the coin). Defining, quantifying and estimating predictive epistemic uncertainty is an active field of research that encompasses many approaches and many methods (see [Hüllermeier and Waegeman, 2021, Lockwood and Si, 2022]). In this work, we take the common approach for quantifying epistemic uncertainty as the variance in a probability distribution of predictions that are consistent with observations $\text{Var}_X(X|s_t) = \mathbb{V}_X[X|s_t]$.

As for estimating epistemic uncertainty, two standard approaches are the distributional approach and the proxy-based approach. The distributional approach approximates a probability distribution over possible predictions with respect to the agent's experiences, while the proxy-based approach aims to directly predict a measure for *novelty* of experiences. Two reliable and lightweight methods for novelty-based epistemic uncertainty estimation are Random Network Distillation (RND) [Burda et al., 2019] and state-visitation counting. RND evaluates novelty as the difference between the prediction

of a randomly initialized untrained target network ψ' and a to-be trained network ψ with a similar architecture. The network ψ is trained to match the predictions of the target network for the observed states (or state-action pairs) with MSE loss $L_{rnd}(\psi(s_t, a_t), \psi'(s_t, a_t))$. Novel observations are expected to produce unpredictable outputs from the target network, and thus the difference between the prediction of the target network and the trained network serves as a proxy-measure for novelty. These methods encapsulate the epistemic uncertainty in a local prediction: for example, uncertainty in prediction of reward or next state. Estimating epistemic uncertainty in value predictions that need to contain the uncertainty that propagates from future information is a different matter. One method to estimate value uncertainty is the Uncertainty Bellman Equation [UBE, O'Donoghue et al., 2018]. UBE approximates an upper bound on the epistemic uncertainty in value (here interpreted as variance of the Q-value) as the sum of local uncertainties $\sigma^2(s_t, a_t)$ that are associated with the decisions a_t at states s_t :

$$U^\pi(s_t) := \mathbb{E}_\pi \left[\sum_{i=0}^{\infty} \gamma^{2i} \sigma^2(s_{t+i}, a_{t+i}^\pi) \right] = \mathbb{E}_\pi \left[\sum_{i=0}^{n-1} \gamma^{2i} \sigma^2(s_{t+i}, a_{t+i}^\pi) + \gamma^{2n} U^\pi(s_{t+n}) \right].$$

In other words, UBE proposes to approximate the value uncertainty as the sum of twice-discounted local uncertainties and learn it with (possibly n -step) TD targets in a similar manner to value learning.

3 Deep Exploration by Planning with Epistemic Uncertainty

In order to enable estimation of epistemic uncertainty in the predictions of value at the root of the MCTS planning tree we need two mechanisms. (i) A mechanism to estimate the epistemic uncertainty associated locally with predictions of state, reward and value in the planning tree. (ii) A mechanism for propagating the uncertainty in the tree. We assume access to mechanism (i) and develop mechanism (ii) in Section 3.1. We follow with an exploration approach that relies on the epistemic uncertainty to plan for an exploratory objective by modifying the UCT formula, in Section 3.2. In Section 3.3 we discuss challenges with estimating epistemic uncertainty of local predictions in planning as well as possible solutions.

3.1 Propagating Uncertainty in MCTS

At planning step i , selecting a path of length T through a decision tree is equivalent to choosing a sequence of T actions $a_{0:T-1}^i$ that start at node $\hat{s}_0^i = g(s_t)$ and end up in a leaf node \hat{s}_T^i . In standard MCTS a deterministic model predicts the encountered rewards r_k^i in nodes \hat{s}_k^i , $0 \leq k < T$, and the estimated value v_T^i at the leaf \hat{s}_T^i is predicted by a neural network or a Monte-Carlo rollouts with the same model. The values and rewards are used to update the n -step discounted return ν_k^i of each node \hat{s}_k^i on the selected path:

$$\nu_k^i := \sum_{j=k}^{T-1} \gamma^{j-k} r_j^i + \gamma^{T-k} v_T^i = r_k^i + \gamma \nu_{k+1}^i, \quad 0 \leq k < T, \quad \nu_T^i = v_T^i. \quad (4)$$

Where γ^{j-k} is the discount factor to the power of $j - k$ and the superscript i is indexing the planning step. Our following analysis is done per planning step i and we will drop the index i for the sake of readability. If the model that produces states, rewards and / or values cannot be fully trusted r_k and v_T can be formulated as random variables in a Markov chain that is connected by random state-variables. To clarify notation, we will refer to these as random states \hat{S}_k , rewards R_k , values V_k and returns \mathcal{V}_k . In exploration, paths that lead to under-explored states or states where the model is not reliable yet should be incentivized. In line with the optimistic exploration literature, we aim to incentivize choosing actions in the environment associated with paths in the planning tree that have *uncertain* returns \mathcal{V}_0 in order to both improve the model as well as find high-reward interactions. For this we need to estimate the variance $\mathbb{V}_{\mathcal{V}_0}[\mathcal{V}_0|s_t, a_{0:T-1}]$ of the return along a selected path $a_{0:T-1}$, starting with state s_t . To improve readability, we will omit in the following the condition on actions and starting state, for example, $\mathbb{V}_{\mathcal{V}_0}[\mathcal{V}_0] \equiv \mathbb{V}_{\mathcal{V}_0}[\mathcal{V}_0|s_t, a_{0:T-1}]$.

We will begin by deriving the mean and variance of the distribution of state-variables in the Markov chain for a given sequence of actions $a_{0:T-1}$. Let us assume we are given a differentiable transition function $f(\hat{S}_k, a_k) := \mathbb{E}_{\hat{S}_{k+1}}[\hat{S}_{k+1}|\hat{S}_k, a_k] \in \mathbb{R}^{|\hat{\mathcal{S}}|}$, which predicts the conditional expectation over the next state, and a differentiable uncertainty function $\Sigma(\hat{S}_k, a_k) := \mathbb{V}_{\hat{S}_{k+1}}[\hat{S}_{k+1}|\hat{S}_k, a_k] \in \mathbb{R}^{|\hat{\mathcal{S}}| \times |\hat{\mathcal{S}}|}$

that yields the conditional-covariance matrix of the distribution. In DMBRL the assumption that models are differentiable is standard (see Section 2.3). We will use an epistemic uncertainty measure to compute the uncertainty function, but in principle $f(\hat{S}_k, a_k)$ and $\Sigma(\hat{S}_k, a_k)$ could represent the mean and variance of a distribution containing any kind of uncertainty, epistemic or otherwise. We assume that the mean \hat{s}_0 of the first state-variable \hat{S}_0 is given as an encoding function $\hat{s}_0 = \mathbb{E}_{\hat{S}_0}[\hat{S}_0|s_t] = g(s_t)$, like in MuZero. The mean \hat{s}_{k+1} of a later state-variable \hat{S}_{k+1} can be approximated with a first order Taylor expansion around the previous mean $\hat{s}_k := \mathbb{E}_{\hat{S}_k}[\hat{S}_k]$:

$$\begin{aligned}\hat{s}_{k+1} &:= \mathbb{E}_{\hat{S}_{k+1}}[\hat{S}_{k+1}] = \mathbb{E}_{\hat{S}_k}[\mathbb{E}_{\hat{S}_{k+1}}[\hat{S}_{k+1}|\hat{S}_k, a_k]] = \mathbb{E}_{\hat{S}_k}[f(\hat{S}_k, a_k)] \quad (5) \\ &\approx \mathbb{E}_{\hat{S}_k}[f(\hat{s}_k, a_k) + (\hat{S}_k - \hat{s}_k)^\top \nabla_{\hat{s}} f(\hat{S}, a_k)|_{\hat{S}=\hat{s}_k}] = f(\hat{s}_k, a_k).\end{aligned}$$

In other words, under the assumption that the model f predicts the *expected* next state we reinterpret the original latent state \hat{s}_k as the mean of the uncertain state $\mathbb{E}_{\hat{S}_k}[\hat{S}_k]$.

To approximate the covariance $\Sigma_{k+1} := \mathbb{V}_{\hat{S}_{k+1}}[\hat{S}_{k+1}]$ or *the total uncertainty associated with state variable* \hat{S}_{k+1} we need the *law of total variance*. The law of total variance states that for two random variables X and Y holds $\mathbb{V}_Y[Y] = \mathbb{E}_X[\mathbb{V}_Y[Y|X]] + \mathbb{V}_X[\mathbb{E}_Y[Y|X]]$ (see Appendix A for a proof in our notation). Using the law of total variance and again a first order Taylor approximation around the previous mean state \hat{s}_k :

$$\begin{aligned}\Sigma_{k+1} &:= \mathbb{V}_{\hat{S}_{k+1}}[\hat{S}_{k+1}] = \underbrace{\mathbb{E}_{\hat{S}_k}[\mathbb{V}_{\hat{S}_{k+1}}[\hat{S}_{k+1}|\hat{S}_k, a_k]]}_{\Sigma(\hat{s}_k, a_k)} + \underbrace{\mathbb{V}_{\hat{S}_k}[\mathbb{E}_{\hat{S}_{k+1}}[\hat{S}_{k+1}|\hat{S}_k, a_k]]}_{\mathbf{J}_f(\hat{s}_k, a_k) \Sigma_k \mathbf{J}_f(\hat{s}_k, a_k)^\top}. \quad (6)\end{aligned}$$

Note that $f(\hat{S}_k, a_k) - \mathbb{E}_{\hat{S}_k}[f(\hat{S}_k, a_k)] \approx (\hat{S}_k - \hat{s}_k)^\top \nabla_{\hat{S}} f(\hat{S}, a_k)|_{\hat{S}=\hat{s}_k} =: (\hat{S}_k - \hat{s}_k)^\top \mathbf{J}_f(\hat{s}_k, a_k)^\top$, where $\mathbf{J}_f(\hat{s}_k, a_k)$ denotes the Jacobian matrix of function f at mean state \hat{s}_k and action a_k .

Using these state statistics, we can derive the means and variances of causally connected variables like rewards R_k and values V_T . We assume that the conditional reward distribution has conditional mean $r(\hat{S}_k, a_k) := \mathbb{E}_{R_k}[R_k|\hat{S}_k, a_k]$ and conditional variance $\sigma_R^2(\hat{S}_k, a_k) := \mathbb{V}_{R_k}[R_k|\hat{S}_k, a_k]$, and that the conditional value distribution has conditional mean $v(\hat{S}_T) := \mathbb{E}_{V_T}[V_T|\hat{S}_T]$ and conditional variance $\sigma_V^2(\hat{S}_T) := \mathbb{V}_{V_T}[V_T|\hat{S}_T]$. Analogous to above we can derive:

$$r_k := \mathbb{E}_{R_k}[R_k] \approx r(\hat{s}_k, a_k), \quad \mathbb{V}_{R_k}[R_k] \approx \sigma_R^2(\hat{s}_k, a_k) + \mathbf{J}_r(\hat{s}_k, a_k) \Sigma_k \mathbf{J}_r(\hat{s}_k, a_k)^\top, \quad (7)$$

$$v_T := \mathbb{E}_{V_T}[V_T] \approx v(\hat{s}_T), \quad \mathbb{V}_{V_T}[V_T] \approx \sigma_V^2(\hat{s}_T) + \mathbf{J}_v(\hat{s}_T) \Sigma_T \mathbf{J}_v(\hat{s}_T)^\top. \quad (8)$$

If we assume that R_k and the n -step return \mathcal{V}_{k+1} from Equation 4 are independent, we can compute

$$\mathbb{E}_{\mathcal{V}_k}[\mathcal{V}_k] = \mathbb{E}_{R_k, \mathcal{V}_{k+1}}[R_k + \gamma \mathcal{V}_{k+1}] = \mathbb{E}_{R_k}[R_k] + \gamma \mathbb{E}_{\mathcal{V}_{k+1}}[\mathcal{V}_{k+1}], \quad \mathbb{E}_{\mathcal{V}_T}[\mathcal{V}_T] = \mathbb{E}_{V_T}[V_T] \quad (9)$$

$$\mathbb{V}_{\mathcal{V}_k}[\mathcal{V}_k] = \mathbb{V}_{R_k, \mathcal{V}_{k+1}}[R_k + \gamma \mathcal{V}_{k+1}] = \mathbb{V}_{R_k}[R_k] + \gamma^2 \mathbb{V}_{\mathcal{V}_{k+1}}[\mathcal{V}_{k+1}], \quad \mathbb{V}_{\mathcal{V}_T}[\mathcal{V}_T] = \mathbb{V}_{V_T}[V_T] \quad (10)$$

We can therefore approximate the variance $\mathbb{V}_{\mathcal{V}_0}[\mathcal{V}_0|s_t, a_{0:T-1}]$ using one forward pass through the selected path computing all \hat{s}_k and Σ_k , starting with the state encoding $\hat{s}_0 = g(s_t)$, and one backwards pass computing $\mathbb{E}_{\mathcal{V}_k}[\mathcal{V}_k]$ and $\mathbb{V}_{\mathcal{V}_k}[\mathcal{V}_k]$. When applying this approach to model-learning algorithms such as MuZero, we interpret the representation g , dynamics f , value v and reward r functions as outputting the conditional means $\hat{s}_0, \hat{s}_k, v_T, r_k$ respectively.

3.2 Planning for Exploration with MCTS

The UCT operator of MCTS takes into account uncertainty about a node’s subtree via the visitation count (see Equation 1) to drive exploration *inside* the planning tree. To drive exploration in the environment, we add the environmental epistemic uncertainty into the UCT formula in a similar manner, as the averaged standard deviation:

$$a_k := \arg \max_a q(\hat{s}_k, a) + \beta \sqrt{\sigma_q^2(\hat{s}_k, a_k)} + 2C \sqrt{\frac{2 \log(\sum_{a'} N(\hat{s}_k, a'))}{N(\hat{s}_k, a_k)}}, \quad (11)$$

where $\beta \geq 0$ is a constant that can be tuned per task to encourage more or less exploration. The term

$$\sigma_q^2(\hat{s}_k, a_k) := \mathbb{V}_{R_k}[R_k] + \frac{1}{N(\hat{s}_k, a_k)} \sum_{i=1}^{N(\hat{s}_k, a_k)} \mathbb{V}_{\mathcal{V}_{k+1}}^i[\mathcal{V}_{k+1}^i] \quad (12)$$

sums the variances computed individually at every backup step i through the node that is reached by executing action a_k in latent state \hat{s}_k using equations 7 and 10. At each backup step i , with actions a_k^i , state means \hat{s}_k^i and covariances Σ_k^i , the variance $\mathbb{V}_{\mathcal{V}_k^i}[\mathcal{V}_k^i]$ is approximated based on equations 10 and 7:

$$\mathbb{V}_{\mathcal{V}_k^i}[\mathcal{V}_k^i] \approx \sigma_R^2(\hat{s}_k^i, a_k^i) + \mathbf{J}_r(\hat{s}_k^i, a_k^i) \Sigma_k^i \mathbf{J}_r(\hat{s}_k^i, a_k^i)^\top + \gamma^2 \mathbb{V}_{\mathcal{V}_{k+1}^i}[\mathcal{V}_{k+1}^i]. \quad (13)$$

At every backup step we compute the variance at the leaf node (equation 8), which is then used to update the parents' variance along the trajectory iteratively using equation 13.

When using other search heuristics such as PUCT or the extension of PUCT used in Gumbel MuZero [Danihelka et al., 2022, Grill et al., 2020] we propose to view the term $q(\hat{s}_k, a) + \beta \sqrt{\sigma_q^2(\hat{s}_k, a_k)}$ as an exploratory-Q-value-estimate (or epistemically-optimistic-Q-value estimate) and use it in place of $q(\hat{s}_k, a)$ to modify the planning objective into the exploratory objective.

Once the MCTS-based search with respect to the exploratory Q-value has completed, action selection in the environment can be done in the same manner as for exploitation. For example, by sampling actions with respect to the visitation counts of each action at the root of the tree as done by the original MuZero.

3.3 Estimating Epistemic Uncertainty in Planning

In reinforcement learning, epistemic uncertainty estimation techniques are used to quantify the *lack of knowledge* (which can also be thought of as *novelty*) the agent has about observed states [Osband et al., 2018, Burda et al., 2019]. These methods translate naturally into planning with deterministic models, when the transition model operates over the true state space of the environment $f : \mathcal{S} \times \mathcal{A} \rightarrow \mathcal{S}$. An example is AlphaZero [Silver et al., 2018], where the true transition model of the environment is used in planning, as is common in RL for board games. When the latent state space $\hat{\mathcal{S}}$ is not identical to the true state space \mathcal{S} , however, novelty estimated in the two spaces can be quite different. The relationship between the latent states and the true states (for example, which losses were used to train the model) determines therefore how well novelty in $\hat{\mathcal{S}}$ reflects novelty in \mathcal{S} . We will motivate this idea with an example.

Consider a model that is not *anchored* at all in the observations/states received from the environment, for example, a model that is trained exclusively to enable predictions of value and reward in planning-space, such as in MuZero [Schrittwieser et al., 2020]. And further, consider the case where an agent that uses such a model is trained in a sparse-reward environment, where only one transition into the goal is rewarded. In such an environment, prior to interacting with the goal there is nothing preventing the agent from abstracting all states as the same latent state: all observed transitions yield the same reward/value and *should* therefore be represented by the same latent state. As a result, all latent states will be associated with the same novelty of zero. We refer to models trained under such circumstances, that is, in sparse reward environments with no anchoring of the latent states to true states/observations, *abstracted models*. To the best of our knowledge, no uncertainty estimation method exists that can reliably estimate the novelty of s based on such abstracted representations \hat{s} . This limits the applicability of E-MCTS to models that are anchored in the state/observation space of the environment, such as models trained with a reconstruction loss. In this work we focus on showing that as long as a reliable source of epistemic uncertainty over \mathcal{S} can be accessed during planning, E-MCTS is effective both to estimate the uncertainty in MCTS, as well as to achieve deep exploration. This epistemic uncertainty does not have to be encoded in a probabilistic model, though, which is one of the strengths of E-MCTS. In the anchored model and true model cases, we therefore use the lightweight non-distributional uncertainty estimator RND (see Section 2.4) over latent state action pair (\hat{s}_k, a_k) as a proxy for the local variance $\sigma_R^2(\hat{s}_k, a_k)$. As RND does not explicitly model covariance matrices, we chose to ignore the uncertainty of the latent state $\Sigma_k := \mathbf{0}$ in our experiments, and show that this choice is sufficient for E-MCTS to significantly improve over a comparable non-planning deep exploration baseline. For the abstracted model case of MuZero, we provide the agent with reliable (but unrealistic) transition uncertainty in the form of state-action visitation counts in the true state space \mathcal{S} , and use it in a similar manner.

To estimate the value uncertainty at the leaf $\sigma_V^2(\hat{s}_T)$ we use UBE (see Section 2.4) for all three model cases. UBE is natural to use in the anchored and true model cases, by simply adding a UBE prediction head u to the Mu/AlphaZero architecture, which approximates $u(\hat{s}_k) \approx U^\pi(s_k)$. In the abstracted model case, UBE suffers from similar challenges to transition-uncertainty estimation but also offers

a solution: training the model through UBE predictions (similar to the way in which the model is trained through predictions of value, see Section 2.3), will force the abstracted model to represent states that lead to novelty differently.

4 Related Work

Plan2Explore [P2E, Sekar et al., 2020] is a previous approach that harnesses planning with learned models and epistemic uncertainty for deep exploration, although not for the standard online-RL setting. P2E pre-trains an exploration policy without access to a reward signal and propagates the epistemic uncertainty associated with the transition model in planning, as intrinsic reward. P2E does not use MCTS, and does not trade off between exploitation and exploration. In contrast, our approach propagates the uncertainty explicitly as variance, enables a trade-off in real time between exploration and exploitation and is applicable to the standard online exploration setting in RL. To estimates local uncertainty in planning with the learned model P2E uses a *latent-disagreement-ensemble* (LDE). The ensemble $[\mu_1, \dots, \mu_n]$ is trained separately from the model, and is trained to predict one-step representation predictions of next state for previous state and action $\mu_i(\hat{s}_k, a_k) = g(s_{k+1})$. The variance within the predictions of the ensemble members is used as an estimate of the epistemic uncertainty associated with the transition (\hat{s}_t, a_t) . LDE relies on the abstracted-states \hat{s}_t not collapsing to similar representations regardless of true state s_t , which cannot be assumed without a reconstruction loss (which is indeed used in P2E), and does not solve the problem we identify in Section 3.3.

Moerland et al. [2020] identify that the further a state is from a terminal state, the more uncertainty should be associated with it in planning, and utilizes this uncertainty to bias search in MCTS. This approach does not explicitly distinguish between epistemic and aleatoric uncertainty, nor does it account for sources of uncertainty other than distance from terminality. POMCP [Silver and Veness, 2010] is an approach that was proposed in order to be able to perform MCTS in large POMDPs. POMCP implicitly introduces uncertainty into MCTS by maintaining a probabilistically modelled Bayesian belief state over the state of the agent, using a particle filter. This approach was extended in POMCPOW [Sunberg and Kochenderfer, 2018] and BOMCP [Mern et al., 2021]. This line of approach does not explicitly utilize epistemic uncertainty to optimize decision making for exploration, but rather improves the UCT operator used in the trajectory selection step to achieve better exploitative decisions. In addition, these methods rely on probabilistic models, and are not applicable for standard MCTS. Antonoglou et al. [2021] extended MuZero to the stochastic setting with Stochastic MuZero (S-MuZero). This approach uses stochastic MCTS, decoupling MCTS nodes into two types of nodes: decision and chance, and learns an explicitly stochastic model with a Vector Quantised Variational AutoEncoder [van den Oord et al., 2017]. This approach is tailored for aleatoric uncertainty, but does not explicitly distinguish between aleatoric and epistemic uncertainty, nor does it directly leverage epistemic uncertainty for exploration.

5 Experiments

To investigate the capacity for deep exploration in a hard-exploration benchmark, we evaluate our approach in BSLITE’s Deep Sea environment [Osband et al., 2020]. The Deep Sea environment encapsulates some of the hardest challenges associated with exploration: there is only one optimal action trajectory. The probability of executing the optimal trajectory through random action selection decays exponentially with the size of the environment. Every transition in the direction of the goal rewards with a negative reward that is negligible with respect to the goal reward but is otherwise the only reward the agent sees, further discouraging exploration in the direction that leads to the optimal reward. Finally, the action mappings are randomized such that the effect of the same action is not the same in every state, preventing the agent from generalizing across actions.

Our implementation of the agents builds on the framework of MuZero as implemented and extended by Ye et al. [2021] in EfficientZero. We evaluate E-MCTS in the Deep Sea environment of size 40 by 40 with three variations of the transition model f :

- (i) A **true** transition model (as in AlphaZero), where the local uncertainty is estimated using RND.
- (ii) An **abstracted** fully-MuZero style model that is trained with the standard MuZero L_v , L_r and L_π losses as well as a UBE loss (see Sections 2.4 and 3.3 and Appendix B.2). The representation function g is trained with the same losses as the transition model (see Section 2.3). RND uncertainty in abstracted models is not reliable (see Section 3.3) and we thus provide this model with state-action

Table 1: Mean and standard deviation of the number of environment steps until the first visitation of the goal transition, for each model and exploration method combination, along with % of seeds that found the goal transition.

	Exploration	Average steps to goal transition \pm STD	% seeds that discovered goal
True Model + RND	E-MCTS	7279 \pm 2430	100%
	Only UBE	19167 \pm 2350	100%
	Uninformed	-	0%
Abstracted Model + Counts	E-MCTS	17871 \pm 8666	100%
	Only UBE	33539 \pm 6796	80%
	Uninformed	-	0%
Anchored Model + RND	E-MCTS	14119 \pm 3727	100%
	Only UBE	24101 \pm 6906	70%
	Uninformed	-	0%

visitation counts.

(iii) An **anchored** transition model that is trained to predict the true transition dynamics of the environment through a direct reconstruction loss L_{re}^k between the model predictions and respective states in the environment (see Appendix B.2). No other losses are used to train the model. A representation function g is an identity in this setting. The local uncertainty is estimated using RND.

In all three transition model variations the reward, value and policy functions are all trained in the MuZero manner. For each model, we compare three exploration methods:

- (i) Our method **E-MCTS**: the agent propagates epistemic uncertainty during planning and plans for an exploratory objective.
- (ii) A deep-exploration baseline which uses **only UBE**. This agent uses MCTS to evaluate the value of actions in the same manner to Alpha/MuZero, and explores by taking the action a_t that maximizes the combination of the Q-values approximated by MCTS q , local uncertainty σ^2 and UBE u :

$$a_t = \arg \max_a q(\hat{s}_0, a_t) + \beta \sqrt{\sigma^2(\hat{s}_0, a_t) + \gamma^2 u(f(\hat{s}_0, a_t))}. \quad (14)$$

(iii) The Alpha/MuZero exploration baseline which is **uninformed** with respect to epistemic uncertainty, and samples actions randomly with probabilities proportionally to the visitations to each action at the root of the planning tree softened by a temperature parameter and noised with Dirichlet noise.

With E-MCTS and only-UBE agents we alternate between two types of training episodes: *exploratory* episodes that follow an exploration policy throughout the episode (such as a policy generated by E-MCTS with an exploratory planning objective), and *exploitative* episodes that follow the standard MuZero reward-maximizing exploitation policy throughout the episode. This enables us to provide the agent with quality exploitation targets to evaluate and train the value and policy functions reliably, while also providing a large amount of exploratory samples, that explore the environment much more effectively and are more likely to encounter high-reward interactions earlier in the agent’s training.

We evaluate the different agents through three metrics: (i) expected undiscounted episodic return vs. interactions with the environment (Figure 1, left), (ii) number of explored state-action pairs vs. interactions with the environment (Figure 1, right) and (iii) first visit to goal transition (Table 1). With the true model and RND uncertainty, E-MCTS outperforms the only-UBE agent significantly both in expected regret as well as efficiency of exploration, which illustrates the benefits of our method with access to the true model (Figure 1, top row, Table 1, first block). With the abstracted model and counts uncertainty, E-MCTS similarly outperforms the only-UBE agent, demonstrating that given access to reliable local uncertainty E-MCTS is both viable as well as very strong in the MuZero-style model-learning case, despite relying on UBE-based learned value uncertainty at the leaves (Figure 1, second row and Table 1, second block).

With the anchored model and RND uncertainty E-MCTS outperforms the only-UBE agent both in average number of steps to the optimal transition (Table 1, third block), as well as expected regret (Figure 1, third row, left). The exploration pace of both agents is comparable until most of the environment is searched (Figure 1, third row, right). However, searching the very last states in Deep Sea requires propagating the uncertainty further and further back and becomes an increasingly challenging problem. In this case, E-MCTS demonstrates increased reliability in uncertainty estimation, resulting in consistent exploration until the environment is fully searched

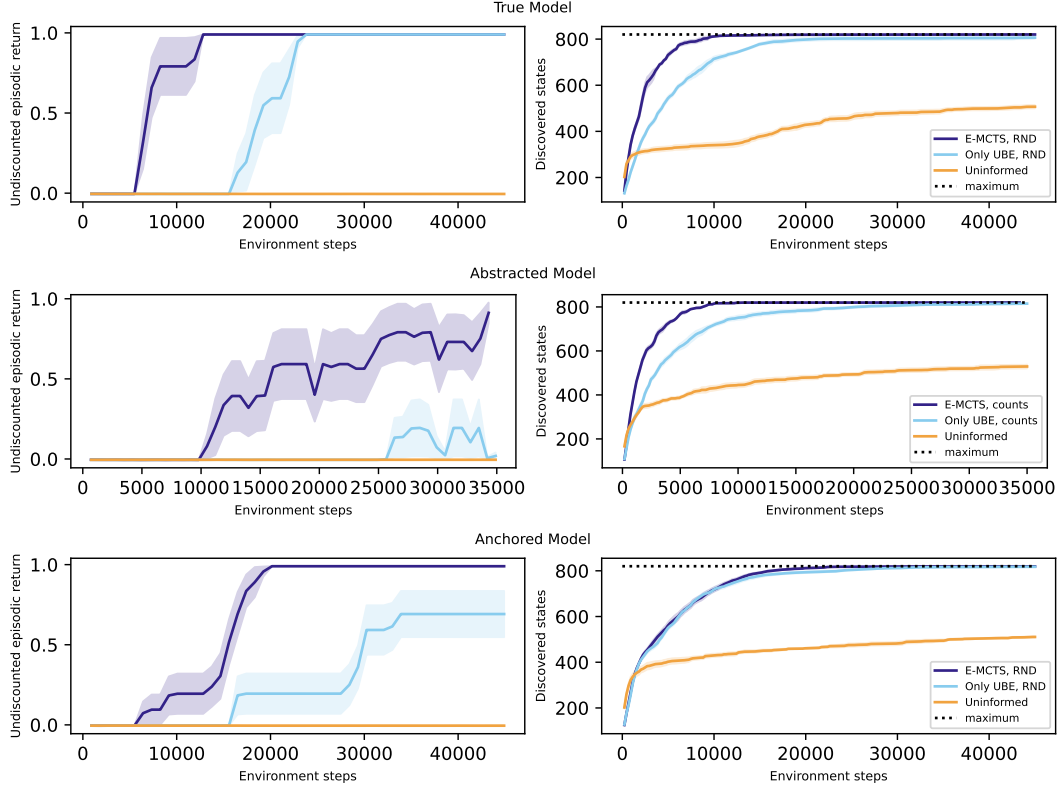


Figure 1: Mean and standard error of the mean of agents using different transition models (rows), and different exploration methods, evaluated against the Deep Sea environment of size 40 by 40. On the left is the learning behavior presented as undiscounted episodic return vs. environment steps. On the right is the exploration behavior presented as number of discovered states vs. environment steps. The performance is averaged over 5 seeds, except in the third row (anchored model), where the performance of the E-MCTS and only-UBE agents is averaged over 10 seeds.

(Figure 1, third row, right, from 15000 steps to 25000 steps) and finding the optimal transition significantly earlier.

6 Conclusions and Future Work

In this work we present E-MCTS, a novel method for incorporating epistemic uncertainty into MCTS. We use E-MCTS to modify the planning objective of MCTS to an exploratory objective, to achieve deep exploration with MCTS-based MBRL agents. We evaluate E-MCTS on the Deep Sea benchmark, which is designed to be a hard exploration challenge, where our method yields significant improvements in state space exploration and uncertainty propagation. In addition, E-MCTS demonstrates the benefits of planning for exploration by empirically outperforming non-planning deep exploration baselines. The framework of E-MCTS provides a backbone for the development of additional approaches to taking advantage of epistemic uncertainty. For example: (i) With E-MCTS, it is possible to plan with a conservative objective by discouraging uncertain decisions to improve reliability in the face of the unknown, which is paramount in the offline-RL setting. (ii) E-MCTS can be used to avoid planning into trajectories that increase epistemic uncertainty in value prediction, with the aim of achieving more reliable planning. (iii) Down-scaling of epistemically-uncertain targets has been used by Lee et al. [2021] and Wu et al. [2021] to improve the learning process of online and offline RL agents respectively. Given the advantages in exploration, it stands to reason that using E-MCTS uncertainties should also improve those approaches. In summary, E-MCTS provides a general framework to estimate and propagate epistemic (and other) uncertainty in tree-based planning like MCTS, which empirically leads to much stronger exploration with a reliable uncertainty measure.

Acknowledgements

We would like to thank Marco Loog, Frank van der Meulen, Itamar Sher, Moritz Zanger, Pascal van der Vaart & Joery de Vries for many fruitful discussions and helpful comments. We acknowledge the use of computational resources of the DelftBlue supercomputer, provided by Delft High Performance Computing Centre (<https://www.tudelft.nl/dhpc>) as well as the INSY cluster. This work was partially supported by the EU Horizon 2020 programme under grant number 964505 (Epistemic AI).

References

Ioannis Antonoglou, Julian Schrittwieser, Sherjil Ozair, Thomas K Hubert, and David Silver. Planning in stochastic environments with a learned model. In *International Conference on Learning Representations*, 2021.

Karl Johan Åström. Optimal control of Markov processes with incomplete state information i. *Journal of Mathematical Analysis and Applications*, 10:174–205, 1965.

Richard Bellman. A Markovian decision process. *Journal of mathematics and mechanics*, 6(5): 679–684, 1957.

Yuri Burda, Harrison Edwards, Amos J. Storkey, and Oleg Klimov. Exploration by random network distillation. In *7th International Conference on Learning Representations, ICLR 2019, New Orleans, LA, USA, May 6-9, 2019*. OpenReview.net, 2019.

Ivo Danihelka, Arthur Guez, Julian Schrittwieser, and David Silver. Policy improvement by planning with Gumbel. In *International Conference on Learning Representations*, 2022.

Jean-Bastien Grill, Florent Altché, Yunhao Tang, Thomas Hubert, Michal Valko, Ioannis Antonoglou, and Rémi Munos. Monte-Carlo tree search as regularized policy optimization. In *International Conference on Machine Learning*, pages 3769–3778. PMLR, 2020.

Eyke Hüllermeier and Willem Waegeman. Aleatoric and epistemic uncertainty in machine learning: An introduction to concepts and methods. *Machine Learning*, 110(3):457–506, 2021.

Diederik P. Kingma and Jimmy Ba. Adam: A method for stochastic optimization. In Yoshua Bengio and Yann LeCun, editors, *3rd International Conference on Learning Representations, ICLR 2015, San Diego, CA, USA, May 7-9, 2015, Conference Track Proceedings*, 2015. URL <http://arxiv.org/abs/1412.6980>.

Levente Kocsis and Csaba Szepesvári. Bandit based Monte-Carlo planning. In *European conference on machine learning*, pages 282–293. Springer, 2006.

Kimin Lee, Michael Laskin, Aravind Srinivas, and Pieter Abbeel. Sunrise: A simple unified framework for ensemble learning in deep reinforcement learning. In *International Conference on Machine Learning*, pages 6131–6141. PMLR, 2021.

Owen Lockwood and Mei Si. A review of uncertainty for deep reinforcement learning. In *Proceedings of the AAAI Conference on Artificial Intelligence and Interactive Digital Entertainment*, volume 18, pages 155–162, 2022.

Amol Mandhane, Anton Zhernov, Maribeth Rauh, Chenjie Gu, Miaozen Wang, Flora Xue, Wendy Shang, Derek Pang, Rene Claus, Ching-Han Chiang, Cheng Chen, Jingning Han, Angie Chen, Daniel J. Mankowitz, Jackson Broshear, Julian Schrittwieser, Thomas Hubert, Oriol Vinyals, and Timothy A. Mann. MuZero with self-competition for rate control in VP9 video compression. *arXiv preprint arXiv:2202.06626*, 2022.

John Mern, Anil Yildiz, Zachary Sunberg, Tapan Mukerji, and Mykel J Kochenderfer. Bayesian optimized Monte-Carlo planning. In *Proceedings of the AAAI Conference on Artificial Intelligence*, volume 35, pages 11880–11887, 2021.

Thomas M Moerland, Joost Broekens, Aske Plaat, and Catholijn M Jonker. The second type of uncertainty in Monte-Carlo tree search. *arXiv preprint arXiv:2005.09645*, 2020.

Thomas M Moerland, Joost Broekens, Aske Plaat, and Catholijn M Jonker. Model-based reinforcement learning: A survey. *Foundations and Trends® in Machine Learning*, 16(1):1–118, 2023.

Brendan O’Donoghue, Ian Osband, Remi Munos, and Volodymyr Mnih. The uncertainty Bellman equation and exploration. In *International Conference on Machine Learning*, pages 3836–3845, 2018.

Ian Osband, John Aslanides, and Albin Cassirer. Randomized prior functions for deep reinforcement learning. *Advances in Neural Information Processing Systems*, 31, 2018.

Ian Osband, Yotam Doron, Matteo Hessel, John Aslanides, Eren Sezener, Andre Saraiva, Katrina McKinney, Tor Lattimore, Csaba Szepesvári, Satinder Singh, Benjamin Van Roy, Richard Sutton, David Silver, and Hado van Hasselt. Behaviour suite for reinforcement learning. In *International Conference on Learning Representations*, 2020. URL <https://openreview.net/forum?id=rygf-kSYwH>.

Christopher D Rosin. Multi-armed bandits with episode context. *Annals of Mathematics and Artificial Intelligence*, 61(3):203–230, 2011.

Julian Schrittwieser, Ioannis Antonoglou, Thomas Hubert, Karen Simonyan, Laurent Sifre, Simon Schmitt, Arthur Guez, Edward Lockhart, Demis Hassabis, Thore Graepel, Timothy Lillicrap, and David Silver. Mastering Atari, Go, Chess and Shogi by planning with a learned model. *Nature*, 588(7839):604–609, 2020.

Ramanan Sekar, Oleh Rybkin, Kostas Daniilidis, Pieter Abbeel, Danijar Hafner, and Deepak Pathak. Planning to explore via self-supervised world models. In *International Conference on Machine Learning*, pages 8583–8592. PMLR, 2020.

David Silver and Joel Veness. Monte-Carlo planning in large POMDPs. *Advances in neural information processing systems*, 23, 2010.

David Silver, Julian Schrittwieser, Karen Simonyan, Ioannis Antonoglou, Aja Huang, Arthur Guez, Thomas Hubert, Lucas Baker, Matthew Lai, Adrian Bolton, Yutian Chen, Timothy Lillicrap, Fan Hui, Laurent Sifre, George van den Driessche, Thore Graepel, and Demis Hassabis. Mastering the game of Go without human knowledge. *Nature*, 550(7676):354–359, 2017.

David Silver, Thomas Hubert, Julian Schrittwieser, Ioannis Antonoglou, Arthur Guez, Marc Lanctot, Laurent Sifre, Dharshan Kumaran, Thore Graepel, Timothy Lillicrap, Karen Simonyan, and Demis Hassabis. A general reinforcement learning algorithm that masters Chess, Shogi, and Go through self-play. *Science*, 362(6419):1140–1144, 2018.

Zachary N Sunberg and Mykel J Kochenderfer. Online algorithms for POMDPs with continuous state, action, and observation spaces. In *Twenty-Eighth International Conference on Automated Planning and Scheduling*, 2018.

Aaron van den Oord, Oriol Vinyals, and Koray Kavukcuoglu. Neural discrete representation learning. In *Advances in Neural Information Processing Systems*, volume 30, 2017.

Yue Wu, Shuangfei Zhai, Nitish Srivastava, Joshua M Susskind, Jian Zhang, Ruslan Salakhutdinov, and Hanlin Goh. Uncertainty weighted actor-critic for offline reinforcement learning. In *International Conference on Machine Learning*, pages 11319–11328. PMLR, 2021.

Weirui Ye, Shaohuai Liu, Thanard Kurutach, Pieter Abbeel, and Yang Gao. Mastering Atari games with limited data. *Advances in Neural Information Processing Systems*, 34:25476–25488, 2021.

A Law of Total Variance

The *law of total variance* for two continuous random variables X and Y can be derived as follows:

$$\begin{aligned}
\mathbb{V}_Y[Y] &= \int (Y - \mathbb{E}_Y[Y])^2 p(Y) dY = \iint (Y - \mathbb{E}_Y[Y])^2 p(X, Y) dX dY \\
&= \iint (Y - \mathbb{E}_Y[Y])^2 p(Y|X) p(X) dX dY = \mathbb{E}_X \left[\mathbb{E}_Y [(Y - \mathbb{E}_Y[Y])^2 | X] \right] \\
&= \mathbb{E}_X \left[\mathbb{E}_Y [(Y - \mathbb{E}_Y[Y|X]) + \mathbb{E}_Y[Y|X] - \mathbb{E}_Y[Y])^2 | X] \right] \\
&= \mathbb{E}_X \left[\underbrace{\mathbb{E}_Y [(Y - \mathbb{E}_Y[Y|X])^2 | X]}_{\mathbb{V}_Y[Y|X]} \right] + 2 \mathbb{E}_X \left[\underbrace{(\mathbb{E}_Y[Y|X] - \mathbb{E}_Y[Y|X]) (\mathbb{E}_Y[Y|X] - \mathbb{E}_Y[Y])}_0 \right] \\
&\quad + \underbrace{\mathbb{E}_X \left[(\mathbb{E}_Y[Y|X] - \mathbb{E}_Y[Y])^2 \right]}_{\mathbb{V}_X[\mathbb{E}_Y[Y|X]]} = \mathbb{V}_X[\mathbb{E}_Y[Y|X]] + \mathbb{E}_X[\mathbb{V}_Y[Y|X]]
\end{aligned}$$

B Implementation Details

B.1 Targets

In MuZero, the value targets v_{t+k}^{MCTS} for the prediction of value of latent state \hat{s}_t^k that matches true state s_{t+k} are computed as an n -step TD target:

$$v_{t+k}^{\text{MCTS}} = \sum_{i=0}^{n-1} \gamma^i r_{t+k+i} + \gamma^n v_{t+k+n}^{\text{MCTS}}$$

Where v_{t+k+n}^{MCTS} can be computed in one of two ways:

- (i) The value of the root of an MCTS tree computed for state s_{t+k+n} .
- (ii) A prediction of the value network v for latent state \hat{s}_{t+k+n}^0 .

Method (i) is expected to result in better value targets, but is more expensive computationally. Method (ii) is significantly cheaper computationally, but might hinder learning through the lack of value improvement (a max operator) on the value bootstrap. We refer to (i) as *root-based targets*.

The UBE target u_{t+k}^{target} for the prediction of value-uncertainty from the UBE head $u(\hat{s}_t^k)$ is computed a similar manner:

$$u_{t+k}^{\text{target}} = \sum_{i=0}^{n-1} \gamma^{2i} \sigma^2(\hat{s}_{t+k+i}^0, a_{t+k+i}) + \gamma^{2n} u_{t+k+n}$$

Analogous to the value target, the bootstrap u_{t+k+n} can be computed in two different ways:

- (i) When E-MCTS is used, the target can be computed similarly to the MuZero value target, as the epistemic uncertainty of the root of an E-MCTS tree computed for state s_{t+k+n} . This tree can plan for an exploitative objective (equation 1) to estimate the uncertainty of the value $V^\pi(s_{t+k+n})$, an exploratory objective (equation 11) to estimate the uncertainty of the value associated with the exploration policy, or even an uncertainty-maximizing objective:

$$a_k := \arg \max_{a_k} \sqrt{\sigma_q^2(\hat{s}_k, a_k)} + 2C \sqrt{\frac{2 \log(\sum_{a'} N(\hat{s}_k, a'))}{N(\hat{s}_k, a_k)}}$$

Where the q term has been dropped entirely as an optimistic bound over the uncertainty to encourage exploration. Similarly, we refer to using as target the E-MCTS uncertainty prediction at the root as a root-based target. In our experiments, when UBE root-based target were used, we have used the uncertainty-maximizing objective.

- (ii) When E-MCTS is not used, the UBE bootstrap u_{t+k+n} is computed as the maximum UBE over possible actions from state s_{t+k+n} :

$$u_{t+k+n} = \max_{a_{t+k+n}} \sigma^2(\hat{s}_{t+k+n}^0, a_{t+k+n}) + \gamma^2 u(f(\hat{s}_{t+k+n}^0, a_{t+k+n}))$$

These targets were used for all UBE-only agents, and for the E-MCTS agents that did not use root-based targets.

In all experiments we have used $n = 1$ (one-step targets) for the UBE targets.

In MuZero, the reward and value predictions $r(\hat{s}_t^k, a_{t+k}), v(\hat{s}_t^k)$ are represented as a discrete probability distribution over a range of discrete values $[-M, M]$, $M \in \mathbb{N}$. To transform the scalar value and reward targets to a categorical representation of the same representation format, a transformation function $\phi(x)$ is used, transforming a real number x into a categorical representation through a linear interpolation between its adjacent integers.

B.2 Losses

The original MuZero algorithm uses three loss functions:

$$\begin{aligned}\mathcal{L}_r &:= \frac{1}{|\mathcal{B}|} \sum_{t \in \mathcal{B}} \sum_{k=0}^{l-1} \phi(r_{t+k})^\top \log r(\hat{s}_t^k, a_{t+k}) \\ \mathcal{L}_v &:= \frac{1}{|\mathcal{B}|} \sum_{t \in \mathcal{B}} \sum_{k=0}^{l-1} \phi(v_{t+k}^{\text{MCTS}})^\top \log v(\hat{s}_t^k) \\ \mathcal{L}_\pi &:= \frac{1}{|\mathcal{B}|} \sum_{t \in \mathcal{B}} \sum_{k=0}^{l-1} \pi^{\text{MCTS}}(s_{t+k})^\top \log \pi(\hat{s}_t^k)\end{aligned}$$

Where $\mathcal{B} \equiv \{s_t, a_t, r_t, s_{t+1}, a_{t+1}, \dots, s_{t+l}\}_{t \in \mathcal{B}}$ is a training batch containing b trajectories of length l sampled from different episodes, r_{t+k} is the true reward observed in the environment, $r(\hat{s}_t^k, a_k), v(\hat{s}_t^k), \pi(\hat{s}_t^k)$ are respectively the reward value and policy predictions for latent state \hat{s}_t^k (and action a_{t+k} when appropriate). $\pi^{\text{MCTS}}(s_{t+k})$ is a discrete probability distribution computed based on the normalized visitation counts to the children of an MCTS root computed at state s_{t+k} (see Equation 3).

In MuZero the gradient from the losses $\mathcal{L}_r, \mathcal{L}_v, \mathcal{L}_\pi$ propagates through the transition model f and are the only learning signal that is used to train the model. For the anchored model (see Section 5) we use an additional reconstruction loss:

$$\mathcal{L}_{re} := \frac{1}{|\mathcal{B}|} \sum_{t \in \mathcal{B}} \sum_{k=0}^{l-1} \|\hat{s}_t^k - s_{t+k}\|^2$$

Which can alternatively be thought of as a consistency loss, where g is the identity function. The mean squared error loss is denoted with \mathcal{L}_{MSE} . To estimate value-uncertainty at the leaves, we train a UBE function u with a UBE loss \mathcal{L}_u :

$$\mathcal{L}_u := \frac{1}{|\mathcal{B}|} \sum_{t \in \mathcal{B}} \sum_{k=0}^{l-1} \phi(u_{t+k}^{\text{target}})^\top \log \hat{u}_t^k$$

The final loss is computed as:

$$\mathcal{L} := \lambda_r \mathcal{L}_r + \lambda_v \mathcal{L}_v + \lambda_\pi \mathcal{L}_\pi + \lambda_u \mathcal{L}_u$$

Where the coefficients $\lambda_r, \lambda_v, \lambda_\pi, \lambda_u$ are used to weigh the relative effects the individual components of the loss have on the learned transition model f . When \mathcal{L}_{re} was used (the anchored model in Section 5), the model parameters of f were affected only by \mathcal{L}_{re} , through a second backwards pass.

B.3 Planning with Random Network Distillation Based Epistemic Uncertainty

We use RND to evaluate the transition uncertainty $\sigma^2(s_t, a_t)$ in planning with the true and anchored models. When the planning is done with a true model, the agent has access to the true states s_{t+k} and using RND to evaluate transition uncertainty over the state action pair (s_{t+k}, a_{t+k}) is natural. When the planning is done with the anchored model, the latent states outputted by the transition model \hat{s}_t^k approximate the true states s_{t+k} which allows us to use RND over (\hat{s}_t^k, a_{t+k}) . In both cases, RND is trained only over the observed transitions (s_{t+k}, a_{t+k}) , not latent state representations (\hat{s}_t^k, a_{t+k}) , to achieve the objective of yielding large RND prediction errors the further the latent state prediction \hat{s}_t^k is from observed state s_{t+k} .

B.4 Planning with Visitation-Counts Based Epistemic Uncertainty

When planning with the abstracted model, we provide the agent with access to two additional mechanisms that are used only for local uncertainty estimation: the true model $F(s_t, a_t)$ of the environment and a state-action visitation counter $C(s_t, a_t)$. During planning, the true transition model follows the planning decisions $a_{t:t+k}$ and keeps track of the true state s_{t+k} . When the agent evaluates the local uncertainty with transition (\hat{s}_t^k, a_{t+k}) the true model provides the matching true state s_{t+k} to the visitation counter, which produces the local uncertainty based on the following computation:

$$\sigma^2(s_{t+k}, a_{t+k}) = \frac{1}{C(s_{t+k}, a_{t+k}) + \epsilon}$$

Where $0 < \epsilon \leq 1$ is a constant and $C(s_{t+k}, a_{t+k})$ counts the number of times the state action pair (s_{t+k}, a_{t+k}) has been observed in the environment. This allows us to evaluate the abstracted-model agent in the presence of a reliable source of local uncertainty. The leaf-value uncertainty $u(\hat{s}_t^k)$ (which is the dominating factor in visited areas of the state space, as $\sigma^2(s_{t+k}, a_{t+k}) \rightarrow 0$ quickly in observed transitions) relies entirely on the learned UBE function u which operates directly on latent states \hat{s}_t^k .

B.5 Separating Exploration from Exploitation

As described in section 5, we execute separate exploration and exploitation episodes, and in principle alternate between the two to provide the agent with exploratory targets that may include new information as well as exploitative targets that reliably evaluate the agent’s policy. In principle, off-policy algorithms can learn stable policies from entirely exploratory data. In practice however, off-policy algorithms are observed to be increasingly unstable the more the data collecting policy differs from the exploitation policy. In addition to that, due to the nature of the n -step TD value targets used by MuZero, the first component of the target $\sum_{i=0}^{n-1} \gamma^i r_{t+k+i}$ is on-policy, which further motivates providing access to on-policy targets as well as exploratory, off-policy targets.

In practice, rather than alternate between exploration and exploitation episodes we run a certain number of episodes in parallel, a certain portion of which are exploitative and the rest are exploratory. During exploration episodes, we do not wish to bias the search in the tree with respect to previously tried actions, but rather only with respect to the combination of value and uncertainty (equation 11). For this reason, we set the policy prediction $\pi(\hat{s}_t^k)$ (see Equation 2) to uniform over all actions, for all \hat{s}_t^k during exploration episodes. In addition, due to the nature of Deep Sea where one "mistake" will prevent the agent from reaching the goal, we also do not use Dirichlet noise in MCTS with the only-UBE and E-MCTS agents.

B.6 Environment Adaptation

To maintain the exploration difficulty of Deep Sea while reducing numerical challenges, we amplify the goal reward from 1 to 10. To limit the challenge of learning a model that can distinguish between approximately N^2 unique states when learning the true dynamics of the environment, while retaining the exploration challenge of searching for one trajectory in a total of 2^N trajectories, we choose environment size $N = 40$, for a $(40, 40)$ grid. To further simplify model learning with the anchored model, the representation function g that was used for the anchored model transforms the observations from 2 dimensional (N, N) one-hot representations to 1 dimensional $(2N)$ representations where the first N entries are a 1-hot vector representing the row and following N entries are a 1-hot vector representing the column. From this perspective, we can view the \mathcal{L}_{re} loss that was used to train the anchored model as a consistency loss between the representation and the state prediction rather than a reconstruction loss. The loss itself is the same loss specified in Appendix B.2.

B.7 Compute

The experiments were run on the Delft Blue and HPC computation clusters, using any of the following GPU architectures: NVIDIA Quadro K2200, Tesla P100, GeForce GTX 1080 Ti, GeForce RTX 2080 Ti and Tesla V100S. Each seed was run on one GPU, and was given access to 100 GB of RAM and 16 CPU cores. Total training time was in the range of 12 to 65 hours per seed, depending on GPU

Table 2: Network architecture hyperparameters

True Model		
Function	Hidden Layers Sizes	Output Layer Size
f	-	-
g	-	-
r	[256, 256]	21
v	[256, 256]	21
u	[256, 256]	21
π	[256, 256]	2
Anchored Model		
Function	Hidden Layers Sizes	Output Layer Size
f	[1024, 1024, 1024]	80
g	-	-
r	[256, 256]	21
v	[256, 256]	21
u	[256, 256]	21
π	[256, 256]	2
Abstracted Model		
Function	Hidden Layers Sizes	Output Layer Size
f	[1024, 1024, 1024]	100
g	[512, 512]	100
r	[128, 128]	21
v	[128, 128]	21
u	[128, 128, 128]	21
π	[128, 128]	2
RND network architecture		
Function	Hidden Layers Sizes	Output Layer Size
ψ	[1024, 1024]	512
ψ'	[512]	512

architecture and whether root-based targets (see Appendix B.1) which significantly increased training time were used or not.

C Network Architecture & Hyperparameters

C.1 Hyperparameter Search

Due to the large number of hyperparameters in the MuZero framework, our optimization process consisted of manual modifications to the hyperparameters used by Ye et al. [2021] with the objective of achieving learning stability on the target environment with the simplest network architectures possible. Two exceptions to this statement are the RND network architecture and scale, and the exploration parameter β .

The RND architecture was designed with the objective of reliably achieving small RND predictions over observed state-action pairs and large predictions over unobserved state-action pairs. The RND scale was tuned with the objective of achieving local uncertainty measures for unobserved state-action pairs that are significantly larger than the minimum reward of Deep Sea.

The β parameter was tuned with the objective that the E-MCTS and only-UBE agents will prioritize exploration of the environment over exploitation until the entire environment has been searched, and was tuned separately for every model.

C.2 Network Architecture

The functions $f, g, r, v, u, \pi, \psi, \psi'$ used fully connected DNNs of varying sizes. The sizes of the hidden layers and output layers are specified in Table 2.

Table 3: Shared across all models and agents

Parameter	Setting	Comment
Stacked Observations	1	
γ	0.995	
Number of simulations in MCTS	50	
Dirichlet noise ratio (ξ)	0.3	
Root exploration fraction	0	
Batch size	256	
Learning rate	0.0005	
Optimizer	Adam [Kingma and Ba, 2015]	
Unroll steps l	5	
Value target TD steps (n_v)	5	
UBE target TD steps (n_u)	1	
value support size	21	
UBE support size	21	
Reward support size	21	
Reanalyzed policy ratio	0.99	See [Ye et al., 2021]
Prioritized sampling from the replay	True	See [Schrittwieser et al., 2020] Appendix G
Priority exponent (α)	0.6	See [Schrittwieser et al., 2020] Appendix G
Priority correction (β_p)	0.4 \rightarrow 1	See [Schrittwieser et al., 2020] Appendix G
Evaluation episodes	8	
Min replay size for sampling	300	
Self-play network updating interval	5	
Target network updating interval	10	

C.3 Hyperparameter Configuration

We detail the full set of hyperparameters in Tables 3 and 4.

Table 4: Specific for models and agents

Parameter	Setting								
	True Model			Abstracted Model			Anchored Model		
	E-MCTS	UBE	Uninf.	E-MCTS	UBE	Uninf.	E-MCTS	UBE	Uninf.
Training steps / environment interactions	45K	45K	45K	35K	35K	35K	45K	45K	45K
Reward loss weight λ_r	1	1	1	1	1	1	1	1	1
Value-loss weight λ_v	0.5	0.5	0.5	0.5	0.5	0.5	0.5	0.5	0.5
Policy-loss weight λ_π	0.5	0.5	0.5	0.5	0.5	0.5	0.5	0.5	0.5
UBE-loss weight λ_u	0.125	0.125	-	0.25	0.25	-	0.125	0.125	-
RND scale	1.0	1.0	-	-	-	-	0.001	0.001	-
Root based targets	False	False	False	True	True	True	False	False	False
Disabled policy in exploration	True	True	False	True	True	False	True	True	False
Number of parallel episodes	2	2	2	2	2	2	2	2	2
Out of are exploration episodes	1	1	-	1	1	-	1	1	-
Exploration coefficient β	10	10	-	1	1	-	10	10	-
Dirichlet noise magnitude ρ	0	0	0.25	0	0	0.25	0	0	0.25